

## Monte Carlo Simulation of Consecutive Implants into SiO<sub>2</sub> Capped Si

Di Li, Shyh-Horng Yang\*, Chuck Machala\*, Li Lin,  
 Al F. Tasch, Brian Hornung\*, Andrei Li-Fatou\*, Sanjay K. Banerjee  
 Microelectronics Research Center, The University of Texas, Austin, Texas 78758,  
 \*Texas Instruments, Dallas, Texas  
 Email: dli@ece.utexas.edu

### Abstract

The low energy as-implanted profile is very sensitive to the cap oxide layer thickness and PAI conditions. In this work, theoretical and experimental studies have been carried out quantitatively to investigate these dependencies. Using ZBL pair-specific inter-atomic potentials in the Monte Carlo ion implantation simulator, UT-MARLOWE, consecutive implants of PAI and PLDD were simulated and above effects were accurately captured.

### Introduction

As integrated circuits continue to scale beyond the 100 nm regime, ultra-shallow junctions are crucial in order to realize desired device performance according to ITRS [1]. To engineer P-type Lightly Doped Drain (PLDD) implant profiles, Pre-Amorphization Implant (PAI) with species such as Sb, provide additional flexibility and is widely used. However, for low energy implants such as PLDD, the as-implanted profiles are very sensitive to the cap oxide layer thickness and PAI conditions. Therefore, developing predictable Monte Carlo models, which can account for these dependencies is desirable for cost efficiency and reducing development cycle time.

In this study, experiments were designed to study these dependencies quantitatively. Based on Ziegler-Biersack-Littmark (ZBL) pair-specific inter-atomic potential [2] and Kinchin-Pease [3] damage model, an Sb implant model was developed and incorporated into UT-MARLOWE [4]. Then, the PAI and PLDD steps were simulated consecutively. The comparisons with experimental data shows that this model is capable of accurately predicting both the impurity and the damage profiles for different PAI and PLDD conditions for different oxide layer thicknesses.

### Model Description and Calibration

The Monte Carlo model in UT-MARLOWE is based on the binary collision approximation (BCA). In other words, the stopping power of the fast moving ions in solids is decoupled into three parts: nuclear stopping, local electronic stopping and non-local electronic stopping. Typically, for low energy and heavy species implants,

nuclear stopping dominates among these three kinds of stopping powers and we need to pay special attention to it. Therefore, instead of ZBL universal potential [5], ZBL pair-specific inter-atomic potential [2] was used for improved accuracy in simulating nuclear stopping power of the fast moving ions. The electronic model mainly follows the ones developed within UT-MARLOWE. In particular, local electronic stopping follows Firsov's electron exchange model [4], while non-local electronic stopping calculates the ion's movement through the potential established by polarization of the surrounding electron sea [4]. To simulate the de-channeling effect caused by the damage accumulation during the implantation process, the modified Kinchin-Pease [6] damage model was used and calibrated (specifically, the recombination factor) for its simplicity, accuracy and computational efficiency.

### Results and Analysis

A set of experiments was designed in order to understand the dependencies of the as-implanted Sb profiles on energy, dose and cap oxide layer thickness, as well as the dependence of as-implanted B and BF<sub>2</sub> profiles on PAI. Chemical Vapor Deposition (CVD) oxide deposition was used to cap (100) single crystal silicon with oxides of different thicknesses for accurate control purpose. For the 0 nm cap oxide wafers, a HF dip was performed to remove any residual oxide, and then all the wafers were kept in nitrogen purge boxes prior to the implants for control purposes. After the implantation and prior to the Rutherford Backscattering Spectroscopy (RBS) measurement, the oxide layer was removed to improve RBS accuracy. The dopant profile dependence on cap oxide layer thickness is shown in Figs. 1-3. A 2nm difference in cap oxide layer thickness (between bare silicon and 2nm oxide cap) could result in more than 10nm difference in the junction depth (at the concentration level of  $1 \times 10^{18} \text{cm}^{-3}$ ) for as-implanted dopant profiles, even for heavy species such as Sb. As the cap oxide layer thickness increases, the dopant profile becomes less sensitive to the cap layer differences. This sensitivity is well captured by the new model when comparing the predicted results with experimental SIMS data in Figs. 1-3. Using the damage profiles predicted by the Sb implant, a second implant is simulated and the simulation results are shown in Figs. 4-5 for B and BF<sub>2</sub>, respectively. Under the same B implant

conditions, with and without PAI implant, could result in more than 35nm difference in the junction depth (at a concentration level of  $1 \times 10^{18} \text{cm}^{-3}$ ) for as-implanted dopant profiles. This dependence is also well predicted by UT-MARLOWE. After performing the PAI, the as-implanted dopant profiles are no longer sensitive to the cap oxide layer thickness even for light species implant such as B, as shown in Figs. 6. This change of sensitivity is predicted very accurately by UT-MARLOWE as well. Throughout these simulations, the defect profiles of PAI implant play an important role. Moreover, they are also crucial in modeling the Transient Enhanced Diffusion (TED) in annealing processes after the implants for providing as-implanted interstitial and vacancy distributions. The comparison of the defect profiles between simulation and RBS for different consecutive implant conditions is shown in Fig. 7 and fairly good agreement is observed. Finally, the Sb implant model based on ZBL pair specific potential is valid for a fairly wide energy range (up to 100keV), dose range ( $5 \times 10^{12} \text{cm}^{-2}$ – $2 \times 10^{14} \text{cm}^{-2}$ ) and for both on and off-axis implants, as shown in Figs. 8-9.

### Conclusion

The Sb implant model has been developed and incorporated into UT-MARLOWE based on ZBL pair-specific inter-atomic potential. Consecutive implants of Sb and B or  $\text{BF}_2$  into  $\text{SiO}_2$  capped single-crystal Si are simulated and the impact of PAI on PLDD and the impact of cap oxide layer thickness on PAI and PLDD are correctly modeled.

### Acknowledgement

This work is supported in part by the Semiconductor Research Corporation and Texas Instruments. The authors would like to thank Dr. James Ziegler for providing pair-specific inter-atomic potential coefficients.

### References

- [1]. *International Technology Roadmap for Semiconductors*, (Semiconductor Industry Association, San Jose, CA, 1999).
- [2]. J. F. Ziegler, Private communication.
- [3]. G. H. Kinchin and R. S. Pease, "The displacement of atoms in solids by radiation", *Rep. Progr. Phys.*, vol. 18, p. 1, 1955.
- [4]. S. J. Morris, B. Obradovic, S. H. Yang and A. F. Tasch, "Modeling of boron, phosphorus, and arsenic implants into single-crystal silicon over a wide energy range (few keV to several MeV)", *IEDM Technical Digest*, 1996.
- [5]. J. F. Ziegler, J. P. Biersack, and U. Littmark, "The stopping and range of ions in silicon", vol. 1., *Pergamon Press*.
- [6]. G. Wang, "Computationally efficient models for Monte Carlo ion implantation simulation in silicon", M. S. Thesis, The University of Texas, 1997, Austin, TX.

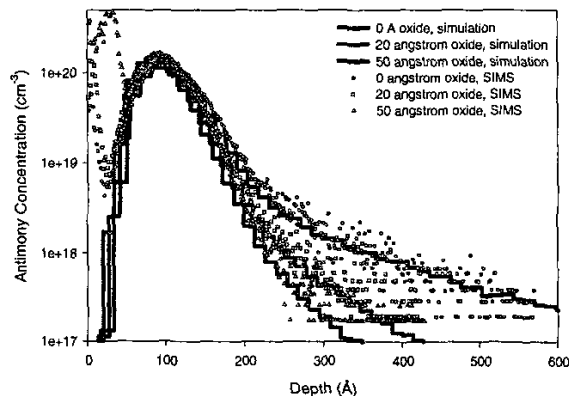


Fig. 1. Comparison between model prediction and SIMS. Implant condition: Sb, 10keV,  $10^{14} \text{cm}^{-2}$ , on-axis.

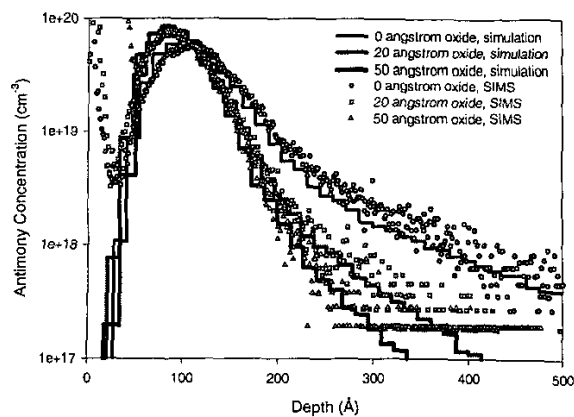


Fig. 2. Comparison between model prediction and SIMS.  
Implant condition: Sb, 10keV,  $6 \times 10^{13} \text{ cm}^{-2}$ , on-axis.

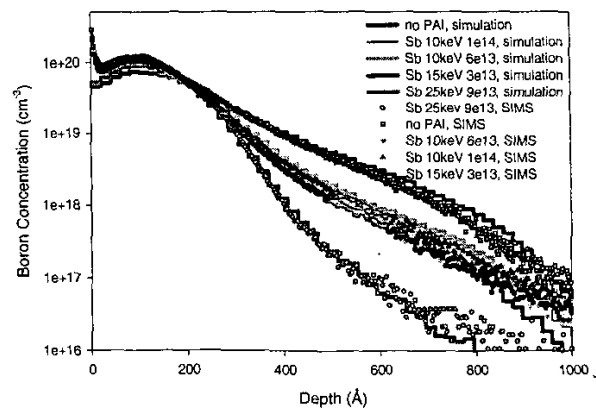


Fig. 4. Comparison between model prediction and SIMS.  
Implant condition: B, 3keV,  $2 \times 10^{14} \text{ cm}^{-2}$ , on-axis, through 2nm oxide.

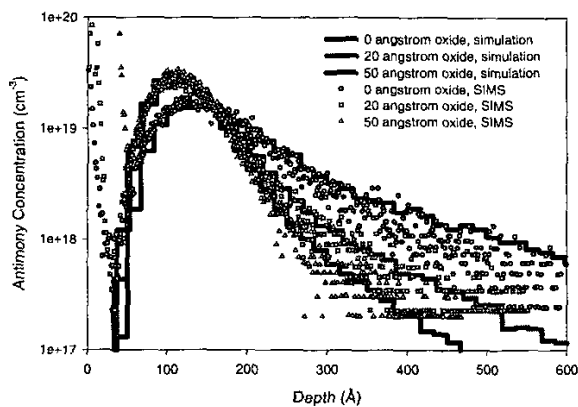


Fig. 3. Comparison between model prediction and SIMS.  
Implant condition: Sb, 15keV,  $3 \times 10^{13} \text{ cm}^{-2}$ , on-axis.

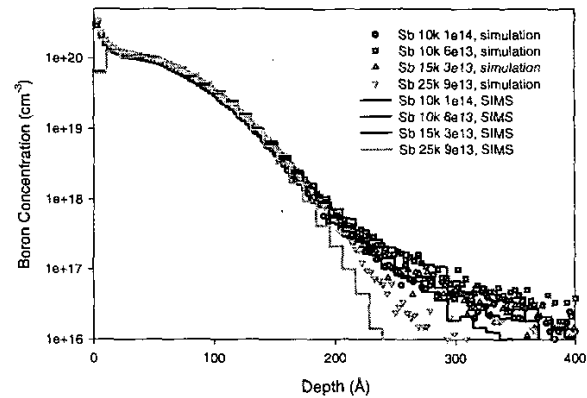


Fig. 5. Comparison between model prediction and SIMS.  
Implant condition:  $\text{BF}_2$ , 5keV,  $10^{14} \text{ cm}^{-2}$ , on-axis, through 2nm oxide.

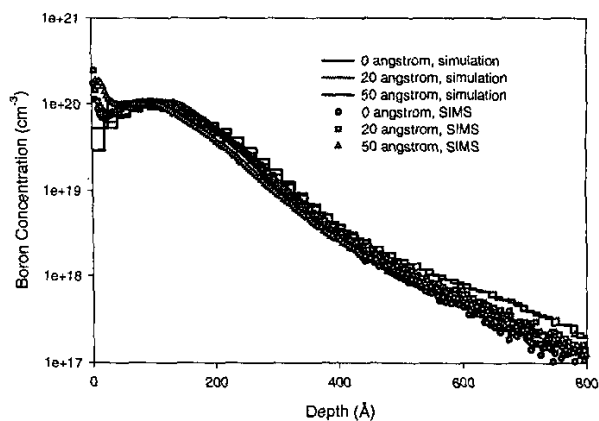


Fig. 6. Comparison between model prediction and SIMS.  
Implant condition: B, 3keV,  $2 \times 10^{14} \text{ cm}^{-2}$ , on-axis 10k 1e14

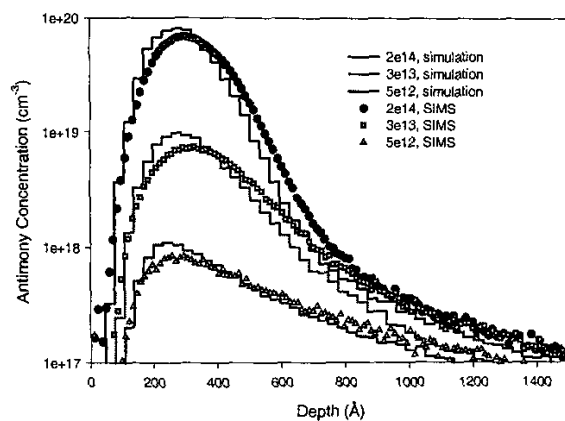


Fig. 8. Comparison between model prediction and SIMS.  
Implant condition: Sb, 50keV, on-axis, through 1.6nm oxide.

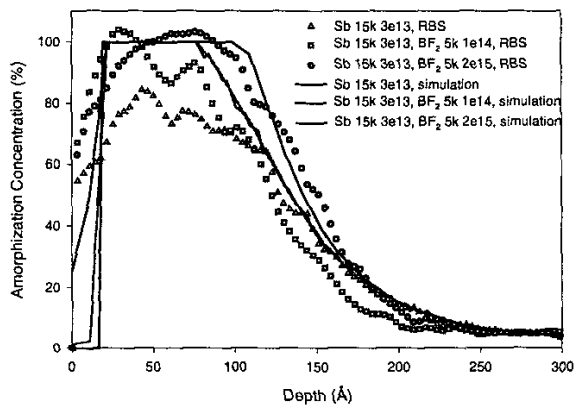


Fig. 7. Comparison between model prediction and RBS.  
Implant condition: on-axis, through 2nm oxide.

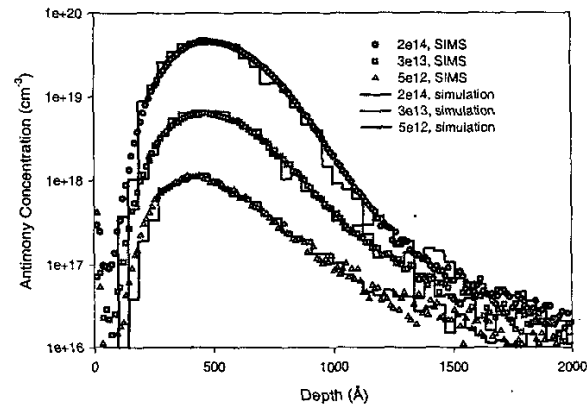


Fig. 9. Comparison between model prediction and SIMS.  
Implant condition: Sb, 100keV, off-axis, through 1.6nm oxide.